Stability of Colloidal Quasicrystals

A. R. Denton[1,*] and H. Löwen[1,2,†]

[1]*Institut für Festkörperforschung, Forschungszentrum Jülich, D-52425 Jülich, Germany*
[2]*Institut für Theoretische Physik II, Universität Düsseldorf, D-40225 Düsseldorf, Germany*
(Received 6 March 1998)

Freezing of charge-stabilized colloidal suspensions and relative stabilities of crystals and quasicrystals are studied using thermodynamic perturbation theory. Macroion interactions are modeled by effective pair potentials combining electrostatic repulsion with polymer depletion or van der Waals attraction. Comparing free energies—counterion terms included—for elementary crystals and rational approximants to icosahedral quasicrystals, parameters are identified for which *one-component* quasicrystals are stabilized by a compromise between packing entropy and cohesive energy. [S0031-9007(98)06552-1]

PACS numbers: 82.70.Dd, 05.70.Fh, 61.44.Br, 83.70.Hq

Suspensions of mesoscopic-sized (1–1000 nm) colloidal particles dispersed in a fluid medium are of both practical and fundamental interest [1]. Beyond traditional relevance to the chemical, food, and pharmaceutical industries, the remarkable mechanical, thermal, and optical properties of these typically soft materials raise intriguing prospects for novel applications, such as optical switching devices [2]. Recent scientific interest has been driven largely by advances in sample preparation, scattering, and imaging techniques [3]. As well-characterized models of atomic systems, colloidal suspensions offer valuable insight into the basic link between microscopic interparticle interactions and macroscopic phase behavior in condensed matter. More so than in atomic systems, colloidal interactions are eminently tunable through experimental control of particle size, charge, and surface chemistry, as well as properties of the suspending medium, such as polarizability and salt concentration. A correspondingly rich variety of thermodynamic phases has been observed, including the vapor, liquid, crystal, and glass phases common to atomic systems. A notable exception is the quasicrystal phase, which to date is known to exist only in certain binary and ternary metallic alloys [4]. The purpose of this Letter is to demonstrate, using general statistical mechanical methods, the possibility of thermodynamically stable *one-component* colloidal quasicrystals. If experimentally observed, such systems would represent a fundamentally new type of colloidal order and permit the first real-space imaging of quasicrystals.

We focus specifically on suspensions of charged spherical colloidal macroions and oppositely charged counterions dispersed in a deionized (salt-free) solvent. The macroions are modeled as hard spheres of diameter σ and uniform surface charge Ze, the counterions as point particles of elementary charge e, and the solvent as a continuous medium of dielectric constant ϵ. Charge neutrality relates the average macroion and counterion number densities via $Z\rho_m = \rho_c$. Electrostatic interactions between charged macroions in suspension are commonly modeled by an effective hard-sphere/screened-Coulomb pair potential:

$$\phi_{\mathrm{el}}(r) = \frac{Z^2 e^2}{\epsilon}\left[\frac{\exp(\kappa\sigma/2)}{1+\kappa\sigma/2}\right]^2 \frac{\exp(-\kappa r)}{r}, \qquad r > \sigma,$$
$$= \infty, \qquad r < \sigma, \tag{1}$$

where r is the separation between macroion centers and $\kappa = \sqrt{4\pi Z e^2 \rho_m/\epsilon k_B T}$ is the Debye screening constant. Equation (1) was first derived in the dilute regime by Derjaguin, Landau, Verwey, and Overbeek [5]. The screened-Coulomb form has since been shown to be accurate also for concentrated suspensions, with Z replaced by an effective charge [6]. At finite macroion volume fractions $\eta = (\pi/6)\rho_m\sigma^3$, the volume available to the counterions is smaller than the total volume V by a factor of $(1-\eta)$. As a result, the effective counterion density is increased by a factor of $1/(1-\eta)$, *enhancing* screening [7] according to $\tilde{\kappa} = \sqrt{4\pi Z e^2 \rho_m/\epsilon k_B T(1-\eta)}$. Henceforth, we assume an electrostatic potential of the form of Eq. (1), but with this modified screening constant.

Aside from electrostatic repulsions, interactions between macroions also can include an attractive component. Attractions may arise, for example, in the presence of free (nonadsorbing) polymer via a polymer-depletion mechanism [8]. For macroion surface-surface separations smaller than the characteristic polymer coil diameter, depletion of polymer from the intervening space creates an osmotic pressure imbalance drawing the macroions together. The attractive energy is directly proportional to the polymer osmotic pressure Π_p and the mutual overlap of excluded volume shells. For coils of sufficiently small radius of gyration R_g relative to σ, the effect is described by a pair potential that is nonzero only in the range $\sigma < r < \sigma + 2R_g$, where it has the form [8]

$$\phi_{\mathrm{dep}}(x) = -c\left[1 - \frac{3x}{2(1+\xi)} + \frac{1}{2}\left(\frac{x}{1+\xi}\right)^3\right], \tag{2}$$

with $x = r/\sigma$, $\xi = 2R_g/\sigma$, and $c = (\pi/6)\Pi_p\sigma^3(1 + \xi)^3$. For size ratios $\xi > 0.16$, triplet overlaps entail three-body interactions. However, for $\xi \simeq 0.25$ (our case below) these are small enough to be ignored [9]. Attractions also may arise from fluctuating dipole-dipole forces, as described by the London–van der Waals pair potential [5]

$$\phi_{\mathrm{vdW}}(x) = -\frac{A}{6}\left[\frac{1}{2x^2} + \frac{1}{2(x^2 - 1)} + \ln\left(1 - \frac{1}{x^2}\right)\right], \tag{3}$$

where the Hamaker constant A is related to the macroion and solvent polarizabilities (refractive indices). The negative divergence at contact ($r = \sigma$) can cause irreversible coagulation unless the macroions are stabilized, e.g., sterically by adsorbing or grafting a layer of polymer to their surfaces. For simplicity, we model this by a cutoff at a distance $r = R_c$, roughly 5%–10% larger than σ.

Figure 1 depicts effective macroion-macroion pair potentials that combine electrostatic repulsion with each of the two types of attraction discussed above. The length scales of the interactions are set by the macroion core diameter, the polymer coil radius (or van der Waals cutoff distance), and the Bjerrum length $\lambda_B \equiv e^2/\epsilon k_B T$ (at temperature T). These pair potentials are now taken as input to a statistical mechanical theory for the Helmholtz free energy. The macroion contribution to the free energy is determined by means of thermodynamic perturbation theory [10]. (An earlier such study by Gast *et al.* [11] considered freezing only into an fcc crystal.) The theory proceeds by splitting the pair potential into short-range reference and longer-range perturbation potentials. The natural separation here is into a hard-sphere (HS) reference potential $\phi_{\mathrm{HS}}(r)$ and a perturbation potential $\phi_p(r)$ that combines an attractive well with a repulsive barrier and long-range tail. To first order in $\phi_p(r)$, the macroion free energy separates correspondingly into reference and perturbation terms:

$$F_m[\rho_m(\mathbf{r})] = F_{\mathrm{HS}}[\rho_m(\mathbf{r})] + 2\pi\rho_m N_m \times \int_0^\infty dr'\, r'^2 g_{\mathrm{HS}}(r'; [\rho_m(\mathbf{r})])\phi_p(r'), \tag{4}$$

$N_m = \rho_m V$ being the macroion number, and $F_{\mathrm{HS}}[\rho_m(\mathbf{r})]$ and $g_{\mathrm{HS}}(r; [\rho_m(\mathbf{r})])$ the free energy and radial distribution function (RDF), respectively, of the HS reference system, both dependent on the *equilibrium* macroion density distribution $\rho_m(\mathbf{r})$. Accuracy of first-order perturbation theory is assured if fluctuations in the total perturbation energy remain small relative to $k_B T$ [10], a condition generally well satisfied here, where variations in $\phi(r)$ are small for distances over which the RDF varies appreciably.

For the fluid phase, with spatially constant macroion density, the macroion free energy is calculated via the uniform limit $[\rho_m(\mathbf{r}) \to \rho_m]$ of Eq. (4), using the essentially exact Carnahan-Starling and Verlet-Weis forms [10] for $F_{\mathrm{HS}}(\rho_m)$ and $g_{\mathrm{HS}}(r; \rho_m)$, respectively. For the solid phase, classical density-functional methods [12] are applied. The reference free energy is obtained by minimizing a *functional* $\mathcal{F}_{\mathrm{HS}}[\rho_m(\mathbf{r})]$ with respect to the macroion density distribution $\rho_m(\mathbf{r})$, or in practice the width parameter α in the Gaussian parametrization

$$\rho_m(\mathbf{r}) = \left(\frac{\alpha}{\pi}\right)^{3/2} \sum_{\mathbf{R}} \exp(-\alpha|\mathbf{r} - \mathbf{R}|^2), \tag{5}$$

the sum running over the lattice sites $\mathbf{R}$ of a specified solid structure. For nonoverlapping Gaussians, the configurational entropy (ideal-gas) part of the functional is given exactly by $\mathcal{F}_{\mathrm{id}}/N_m k_B T = (3/2)\ln(\alpha\sigma^2/\pi) - 5/2$. The excess part is determined by means of the modified weighted-density approximation (MWDA) [13], which reasonably describes HS solids. This maps the excess part of $\mathcal{F}_{\mathrm{HS}}[\rho_m(\mathbf{r})]/N_m$ onto its fluid counterpart, evaluated at an effective density, via $\mathcal{F}_{\mathrm{ex}}^{\mathrm{MWDA}}[\rho_m(\mathbf{r})]/N_m = f_{\mathrm{ex}}(\hat{\rho})$, where f_{ex} is the fluid excess free energy per particle and $\hat{\rho}$ is a weighted average of $\rho_m(\mathbf{r})$ that incorporates exact two-particle correlations and a subset of higher-order correlations. The reference RDF—an angular average of the two-particle density—is calculated using an approach recently proposed by Rascón *et al.* [14]. This corrects the first peak for nearest-neighbor correlations—by fixing the contact value (via the virial theorem), coordination number, and first moment—and treats higher-order peaks in a mean-field fashion. The approximation compares excellently with simulation data for HS crystals and has been successfully applied to Lennard-Jones and square-well solids [14].

The counterion contribution to the free energy is

$$F_c(\rho_m) = F_{\mathrm{OCP}}(\rho_m) - N_m \frac{Z^2 e^2}{2\epsilon} \frac{\tilde{\kappa}}{1 + \tilde{\kappa}\sigma/2}, \tag{6}$$

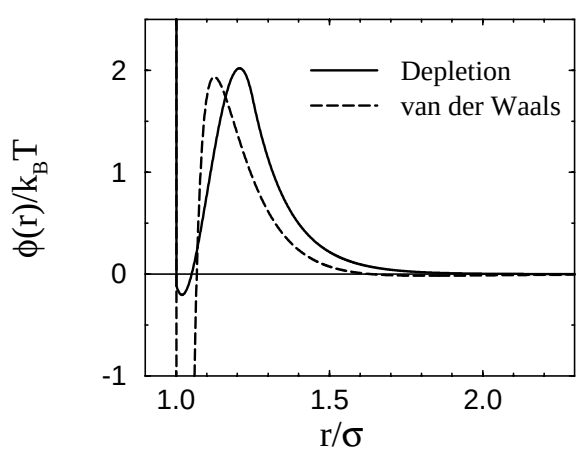

FIG. 1. Effective pair potentials for charge-stabilized colloidal suspensions with $\sigma = 50$ nm, $Z = 150e$. Solid curve: Index-matched suspension mixed with polymer of $R_g/\sigma = 0.125$, $\Pi_p\sigma^3/k_B T = 250$. Dashed curve: Non-index-matched with $R_c/\sigma = 1.058$, $A/k_B T = 25$.

comprising the free energy of a one-component plasma (OCP) of counterions and the interaction of the macroions with their own counterion screening clouds [15,16]. For the weakly coupled OCP of interest here, characterized by coupling parameter $\Gamma \equiv \lambda_B/a_c \ll 1$, where $a_c \equiv [3(1-\eta)/4\pi Z\rho_m]^{1/3}$, it can be shown that the density derivative of the excess part of F_{OCP}, associated with counterion-counterion correlations, is much smaller, by a factor of order $1/Z$, than that of the (entropic) ideal-gas part. Therefore we may ignore correlations [15] and take $F_{\mathrm{OCP}} = k_B TZN_m \ln[\rho_m\sigma^3/(1-\eta)]$. Although independent of macroion structure, the counterion free energy is manifestly state dependent and, under conditions of high charge and low salt, can profoundly influence phase behavior.

Applying the above procedure, we have calculated total free energies for a variety of elementary crystals and model quasicrystals. The crystalline structures examined include face-centered and body-centered cubic (fcc and bcc), tetragonal, orthorhombic, and rhombohedral Bravais lattices, and the hexagonal close-packed (hcp) structure. The model quasicrystalline structures are rational approximants (RA) to icosahedral quasicrystals generated by projecting a six-dimensional hypercubic lattice onto the three-dimensional physical space and approximating, in the perpendicular space, the golden mean τ by a rational number $\tau_n = F_{n+1}/F_n$, where F_n is a term in the Fibonacci sequence. This procedure, together with a one-component occupation of the lattice sites that optimizes packing efficiency [17], yields periodic lattices with large unit cells and local order closely approximating that of aperiodic quasicrystals. The first four RAs, denoted 1/1, 2/1, 3/2, and 5/3, have unit cells containing, respectively, 20, 108, 452, and 1904 atoms and maximum HS volume fractions of 0.5020, 0.6400, 0.6323, and 0.6287 (cf. 0.6288 in the quasiperiodic limit $n \to \infty$ and 0.7405 for fcc and hcp crystals). The RDFs illustrated in Fig. 2 show that nearest-neighbor distances for the RAs are about 5% *shorter* than for the crystals. For computational ease we focus on the 2/1 structure, but check to ensure qualitatively similar results for the higher-order approximants.

From previous work [18], packing efficiency is known to dominate the stability of HS solids, the RAs being always metastable (higher in free energy) relative to the crystals. On the other hand, because of their shorter nearest-neighbor distances, the RAs can gain energetically from short-range attractive interactions. In fact, for potential wells of appropriate depth (a few k_BT) and width (10%–30% of σ), their free energies can be lower than those of simple crystals. As shown above, such attractions can be produced in colloidal systems by adding polymer of appropriate size and concentration [Eq. (2)] or by tuning refractive indices [Eq. (3)].

Assuming a room-temperature, salt-free, aqueous solvent ($\lambda_B = 0.72$ nm), we have surveyed macroion parameters, σ and Z, and parameters defining attractive interactions—ξ and Π_p for index-matched colloid-polymer mixtures, R_c and A for non-index-matched suspensions—computed free energies for each solid structure, and identified parameter combinations tending to favor quasicrystal stability. For illustration, Fig. 3 displays the free energies of a non-index-matched suspension characterized by $\sigma = 50$ nm, $Z = 150e$, $R_c/\sigma = 1.058$, and $A/k_BT = 25$. Hamaker constants of this magnitude, though high for polymeric colloids, are typical for metallic colloids, such as Ag, Au, and Cu. Furthermore, charges of this magnitude correspond to counterion concentrations of order 10^{-3} mol/l, far exceeding the background concentration of 10^{-7} mol/l for H^+ and OH^- ions from the dissociation of water. Relative stabilities of the fluid and competing solid structures are assessed by constructing Maxwell common tangents, ensuring equality of chemical potentials and pressures in coexisting phases. Remarkably, over a range of densities intermediate between dense fluid and close-packed crystals, the quasicrystalline structures are predicted to be thermodynamically stable. The stability can be traced to a competition between two factors,

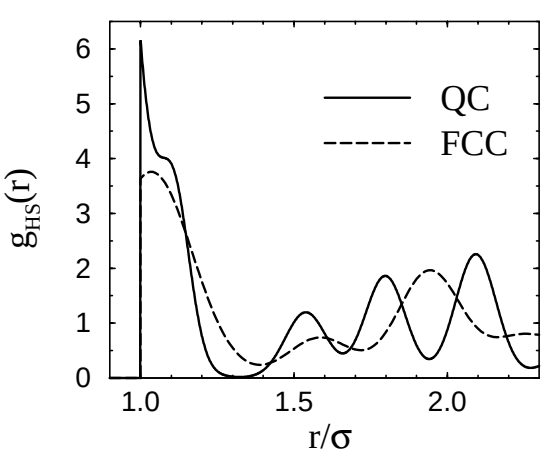

FIG. 2. Radial distribution function of the hard-sphere solid for $\eta = 0.54$. Solid curve: 2/1 rational approximant ($\alpha\sigma^2 = 230$). Dashed curve: fcc crystal ($\alpha\sigma^2 = 120$).

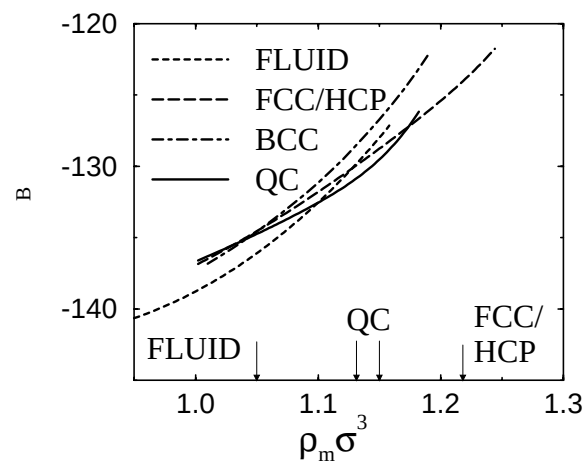

FIG. 3. Helmholtz free energy per unit volume vs macroion density (in reduced units) for a colloidal suspension interacting via pair potential of Fig. 1 (dashed curve).

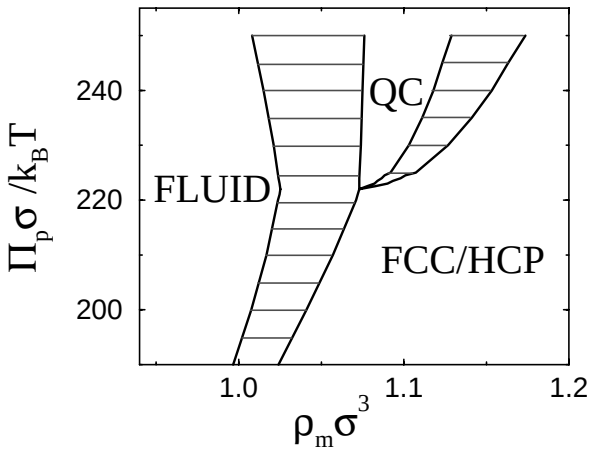

FIG. 4. Phase diagram of polymer osmotic pressure vs macroion density for a colloid-polymer mixture interacting via pair potential of Fig. 1 (solid curve). Horizontal tie lines connect corresponding points on coexistence curves.

namely, packing efficiency, favoring the fcc/hcp crystal, and nearest-neighbor coordination, favoring quasicrystalline order. This is best seen by comparing Figs. 1 and 2 and observing that the attractive well of $\phi(r)$ is more commensurate with the first peak of $g_{\mathrm{HS}}(r)$ for the $2/1$ RA than for the fcc crystal. Stable quasicrystals thus emerge as a compromise between packing entropy and cohesive energy in salt-free colloidal suspensions with a concentrated counterion background.

Applying the same approach to colloid-polymer mixtures, quasicrystalline stability is again predicted for sufficiently high polymer osmotic pressure. Repeating the coexistence analysis over a range of osmotic pressures, we have mapped out phase diagrams in the Π_p-ρ_m plane. A typical example is presented in Fig. 4. At lower osmotic pressures, where the interactions are purely repulsive, the fluid freezes into a close-packed crystal, fcc and hcp being essentially degenerate. Beyond a threshold osmotic pressure, however, freezing occurs into the quasicrystal, which remains stable over a significant range of densities. At the threshold pressure (here $\Pi_p\sigma^3/k_BT \simeq 220$), which we estimate to be near crossover between dilute and semidilute polymer regimes, the fluid, crystal, and quasicrystal coexist at a triple point. At higher densities, packing efficiency prevails and the quasicrystal makes a structural transition to the fcc/hcp crystal. The small relative density differences justify our assumption of equal polymer concentrations in coexisting phases. Finally, we emphasize that the predicted region of quasicrystal stability is robust with respect to variation of parameters, widening and shifting to higher Π_p with increasing σ and Z, and that its existence depends not on specific details, but only the qualitative form, of the interactions.

Summarizing, using thermodynamic perturbation theory, we have investigated freezing transitions and assessed the relative stabilities of crystalline and quasicrystalline solids in charge-stabilized colloidal suspensions. For effective macroion interactions combining electrostatic repulsion with either polymer-depletion or van der Waals attraction, system parameters and thermodynamic states have been identified for which one-component icosahedral quasicrystals are predicted to be thermodynamically stable over a significant range of densities. Such systems and interactions should be experimentally achievable, raising prospects for observation of stable colloidal quasicrystals.

We thank Professor J. Hafner and Dr. A. M. Denton for helpful discussions, and Dr. M. Krajčí and Dr. M. Windisch for supplying the rational approximant structures.

*Electronic address: a.denton@fz-juelich.de
†Electronic address: hlowen@thphy.uni-duesseldorf.de

[1] P. N. Pusey, in *Liquids, Freezing and Glass Transition*, edited by J.-P. Hansen, D. Levesque, and J. Zinn-Justin (North-Holland, Amsterdam, 1991), Session 51.
[2] G. Pan, R. Kesavamoorthy, and S. A. Asher, Phys. Rev. Lett. **78**, 3860 (1997).
[3] Special issue on *Optical Methods and Physics of Colloidal Dispersions*, edited by T. Palberg and M. Ballauff [Prog. Colloid Polym. Sci. **104** (1997)].
[4] D. Shechtman, I. Blech, D. Gratias, and J. W. Cahn, Phys. Rev. Lett. **53**, 1951 (1984); A.-P. Tsai, A. Inoue, and T. Masumoto, Jpn. J. Appl. Phys. **26**, L1505 (1987).
[5] E. J. W. Verwey and J. T. G. Overbeek, *Theory of the Stability of Lyophobic Colloids* (Elsevier, Amsterdam, 1948).
[6] S. Alexander, P. M. Chaikin, P. Grant, G. J. Morales, and P. Pincus, J. Chem. Phys. **80**, 5776 (1984); H. Löwen, P. A. Madden, and J.-P. Hansen, Phys. Rev. Lett. **68**, 1081 (1992); J. Chem. Phys. **98**, 3275 (1993); H. Löwen and G. Kramposthuber, Europhys. Lett. **23**, 673 (1993).
[7] W. B. Russel, in *Theory of Dispersed Multiphase Flow*, edited by R. E. Meyer (Academic, New York, 1981); W. B. Russel and D. W. Benzing, J. Colloid Interface Sci. **83**, 163 (1981).
[8] S. Asakura and F. Oosawa, J. Chem. Phys. **22**, 1255 (1954); A. Vrij, Pure Appl. Chem. **48**, 471 (1976).
[9] A. P. Gast, C. K. Hall, and W. B. Russel, J. Colloid Interface Sci. **96**, 251 (1983); E. J. Meijer and D. Frenkel, Phys. Rev. Lett. **67**, 1110 (1991); J. Chem. Phys. **100**, 6873 (1994).
[10] J.-P. Hansen and I. R. McDonald, *Theory of Simple Liquids* (Academic, London, 1986), 2nd ed.
[11] A. P. Gast, W. B. Russel, and C. K. Hall, J. Colloid Interface Sci. **109**, 161 (1986).
[12] R. Evans, in *Inhomogeneous Fluids*, edited by D. Henderson (Dekker, New York, 1992); D. W. Oxtoby, in *Liquids, Freezing and Glass Transition* (Ref. [1]).
[13] A. R. Denton and N. W. Ashcroft, Phys. Rev. A **39**, 4701 (1989).
[14] C. Rascón, L. Mederos, and G. Navascués, Phys. Rev. E **54**, 1261 (1996); Phys. Rev. Lett. **77**, 2249 (1996).
[15] R. van Roij and J.-P. Hansen, Phys. Rev. Lett. **79**, 3082 (1997).
[16] M. J. Grimson and M. Silbert, Mol. Phys. **74**, 397 (1991).
[17] C. L. Henley, Phys. Rev. B **34**, 797 (1986); M. Krajčí and J. Hafner, Phys. Rev. B **46**, 10 669 (1992).
[18] A. R. Denton and J. Hafner, Europhys. Lett. **38**, 189 (1997); Phys. Rev. B **56**, 2469 (1997).